Hindawi
Journal of Nanomaterials
Volume 2019, Article ID 4101293, 7 pages
https://doi.org/10.1155/2019/4101293

Research Article

Antibacterial Activity of BSA-Capped Gold Nanoclusters against Methicillin-Resistant *Staphylococcus aureus* (MRSA) and Vancomycin-Intermediate *Staphylococcus aureus* (VISA)

Shu-Hua Kuo,[1] Chi-Sheng Chien,[2,3] Chun-Chi Wang,[4,5] and Chi-Jen Shih[6,7]

[1]*Department of Medicinal and Applied Chemistry, Kaohsiung Medical University, Kaohsiung, Taiwan*
[2]*Department of Orthopedics, Chi Mei Medical Center, Tainan, Taiwan*
[3]*Department of Electrical Engineering, Southern Taiwan University of Science and Technology, Tainan, Taiwan*
[4]*School of Pharmacy, College of Pharmacy, Kaohsiung Medical University, Kaohsiung, Taiwan*
[5]*Research Center for Environmental Medicine, Kaohsiung Medical University, Kaohsiung, Taiwan*
[6]*Department of Fragrance and Cosmetic Science, Kaohsiung Medical University, Kaohsiung, Taiwan*
[7]*Department of Medical Research, Kaohsiung Medical University Hospital, Kaohsiung, Taiwan*

Correspondence should be addressed to Chi-Jen Shih; cjshih@kmu.edu.tw

Received 4 March 2019; Revised 2 May 2019; Accepted 5 May 2019; Published 31 July 2019

Academic Editor: Ilaria Fratoddi

The emergence of drug-resistant pathogens and the abuse of antibiotics have posed dominant threats to society. In this study, we propose an antibacterial use of bovine serum albumin-capped gold nanoclusters (BSA-AuNCs) to address the issue. BSA-AuNCs have a great antibacterial activity against MRSA and VISA which is proved by time-killing curves (TKC). The possible antibacterial mechanisms of BSA-AuNCs against MRSA and VISA are confirmed by fluorescence image observation.

1. Introduction

It has driven the rapid emergence of multidrug-resistant (MDR) pathogens due to antibiotic overuse, causing about 700 thousand deaths each year in the world. Pathogens, such as methicillin-resistant *Staphylococcus aureus* (MRSA) and Vancomycin-intermediate *Staphylococcus aureus* (VISA) have been spreading worldwide [1, 2]. The conventional antibacterial agents are practically impossible to inhibit the pathogens; therefore, to develop a new type of antimicrobial material is imperative. However, only three new classes of antibiotics for treatment have been introduced to the market by 2000 [3, 4]. Metal-based antimicrobial agents have gotten more attention since metals cause injures of bacterial cells, such as membrane damage and protein dysfunction [5]. Using metallic nanoparticles as antibacterial materials is potentially capable of preventing patients from the exacerbating MDR infections.

Gold nanoparticles (AuNPs) have better biocompatibility, better thermal and photo stability, and lower cell toxicity to human cells compared to silver nanoparticles (AgNPs) [6–8]. In the study from Connor et al., the K562 leukemia cells after treatment with AuNPs (1 μM, 18 nm, without CTAB) have nearly 100% survival [6]. AuNPs have been used increasingly in the application in interfacing biological recognition and designing of biosensors [9–11].

BSA and its composites owing to good biocompatibility and high photostability have been reported in numerous biological applications, such as immunological labeling [12], tumor imaging [13], biosensor [14], self-assembling [15], and therapeutic applications [16].

Green synthesis of AuNPs by using plants, seed-mediated and honey-mediated, has been developed for 20 years [17–20]. The protein-directed synthesis of AuNPs by using BSA was first published in 2009 [21]. The research introduced a method of elegant, simple, and green synthesis of

the highly fluorescent BSA-AuNCs. Cytotoxicity of BSA-AuNCs has been well discussed both in vitro and in vivo. In this study, the results implied that BSA could prevent cell damage [22]. As a result of it, there are more and more studies which were based on this synthetic method which is applied greatly as a biosensor and photothermal therapy [23–25].

Green synthesis of metal nanoparticles for antibacterial agents has been getting attention [26]. However, until now, scarcely any of the study has been reported in the antibacterial activity against MRD pathogens by using AuNPs and their composites. Green synthesis and antibacterial activity of BSA-AuNCs are discussed in this study.

2. Materials and Methods

2.1. Source of Raw Materials. Bovine serum albumin (BSA, 66 k) and fluorescein isothiocyanate isomer I (FITC) were purchased from Sigma-Aldrich. Gold (III) chloride trihydrate ($HAuCl_4 \cdot 3H_2O$, 49%) was obtained from Acros Organics. L(+)-Ascorbic acid was purchased from ITW Reagents. Tryptic Soy Broth (TSB) was obtained from Acumedia Neogen. Methicillin-resistant *Staphylococcus aureus* (ATCC® 33592™, ATCC® 49476™) and vancomycin-intermediate *Staphylococcus aureus* (ATCC® 700698™, ATCC® 700699™) were purchased from Bioresource Collection and Research Center (BCRC, Taiwan). Dialysis tubing (MWCO 3500 Da) was obtained from Orange Scientific.

2.2. Synthesis of BSA-AuNCs. First, an aqueous solution of 5 ml of $HAuCl_4$ (10 mM) and 5 ml of BSA solution (0.1 wt%) was separately heated at 40°C and vigorously stirred. The warm solution of $HAuCl_4 \cdot 3H_2O$ was added in BSA solution to form BSA-Au^+ complex; then, 0.5 ml NaOH solution (1 M) was added quickly to the mixture. As a result, the solution pH was fixed at 8.0. Subsequently, L(+)-ascorbic acid solution (2 mM, 50 μl) was added as a reductant dropwise into the mixture. The reaction was carried out at 40°C for 24 h, and the color of the solution changed from pale yellow to deep brown. It means that BSA-capped gold nanoclusters (BSA-AuNCs) were formed. While adding $HAuCl_4 \cdot 3H_2O$ in BSA solution, Au (III) would be reduced to form AuNCs after adjusting pH and adding the reductant; then, AuNCs would be sequestered and encapsulated to form BSA-AuNCs by the protein molecules. After BSA encapsulates the AuNCs, the pH is adjusted to 8 and the BSA protein is negatively charged and mutually repelled under alkaline conditions, so that the entire BSA-AuNCs can be dispersed without agglomerating. The as-prepared product was purified by a dialysis tube (3500 Da) and then refrigerated at 4°C for antibacterial experiments, fluorescence imaging, and further measurements.

2.3. Measurement Conditions and Parameters. The particle size and morphology of the BSA-AuNCs were characterized by transmission electron microscopy (TEM, JEM2100, JEOL, Japan) at an accelerating voltage of 200 kV, and the BSA-AuNC solution was diluted 10 times for making TEM samples. Fluorescence spectra of the BSA and BSA-AuNCs were obtained on a fluorescence spectrophotometer (F-7000, HITACHI) with the excitation wavelength at 360 nm, excitation slit at 10 nm, emission slit at 5 nm, PMT voltage at 700 V, and 1200 nm/min scan speed. The quantity of Au was identified by ICP-MS (Thermo Scientific, XSERIES II). Fluorescence images of MRSA and VISA were captured by a confocal laser scanning microscope (cLSM, Olympus, IX-81). The measurement condition of cLSM was used 100x objective and excited at 488 nm. The whole staining session and fluorescence imaging were performed in the dark.

2.4. Bacterial Culture and Antibacterial Experiments. The freeze-dried bacteria of MRSA and VISA were first cultured on Petri dishes for 24 h according to the instruction provided by vendors. The bacteria used in the antibacterial experiments were between the third and fifth generations. Time-killing curves (TKC) were built in the subsequent antibacterial experiments. The third to the fifth generations of bacteria were incubated in TSB solution, then cultured at 32.5°C ± 2.5°C for 24 h. The bacterial solution was fixed at 10^8 CFU/ml as the concentration in 0.5 McFarland units by turbidity. The diluted bacterial solution (5×10^6 CFU/ml, 20 μl) was added to BSA-AuNC solution (200 μl) in a 96-well culture plate, and the final concentration of bacterial solution would be 4.5×10^5 CFU/ml. Because the corpses of the bacteria had also absorbance values, the absorbance value OD_{600} of the solution was positively correlated with the concentration of bacterial solution. The absorbance value OD_{600} of the solution was measured and recorded per hour by a spectrophotometer (INFINITE F50) for 24 h while incubation at 32.5°C ± 2.5°C. The whole experiment was repeated three times.

2.5. Fluorescence Images of MRSA and VISA. The third to the fifth generations of bacteria were treated the same as the abovementioned bacterial culture method. The samples, one contained BSA-AuNCs and the other without BSA-AuNCs (as a control group), were cultured at 32.5°C ± 2.5°C for 24 h. After incubation, the bacteria were centrifuged (4000 rpm, 2 min) and rinsed with PBS buffer three times. The bacteria were fixed with 99% DMSO and again rinsed with PBS buffer three times, then stained with FITC for one hour. After the staining session, excessive FITC was rinsed with PBS buffer and then the bacteria were applied onto a cover glass (in 0.17 mm thickness) and sealed with a glass slice by nail oil.

3. Results and Discussion

3.1. Particle Size and Resonance Characterization of BSA-AuNCs. Figure 1 shows the TEM image of BSA-AuNCs, which indicates that the particles of the AuNCs encapsulated by the BSA are very complete. The shape of the particles is spherical and the average diameter is *ca.* 5 nm. In Figure 2, the blue-emitting control BSA presents a weak broad band at 435 nm and BSA-AuNCs emit an intense red fluorescence at 635 nm. The fluorescence was recorded by a digital camera under a UV lamp (365 nm), as shown in the inset of the Figure 2. The 435 nm emission is in charge of the

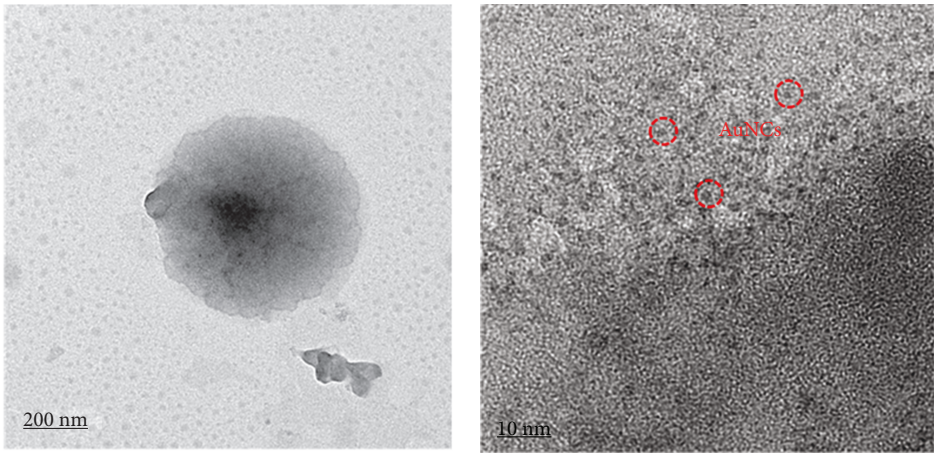

Figure 1: TEM images of BSA-AuNCs.

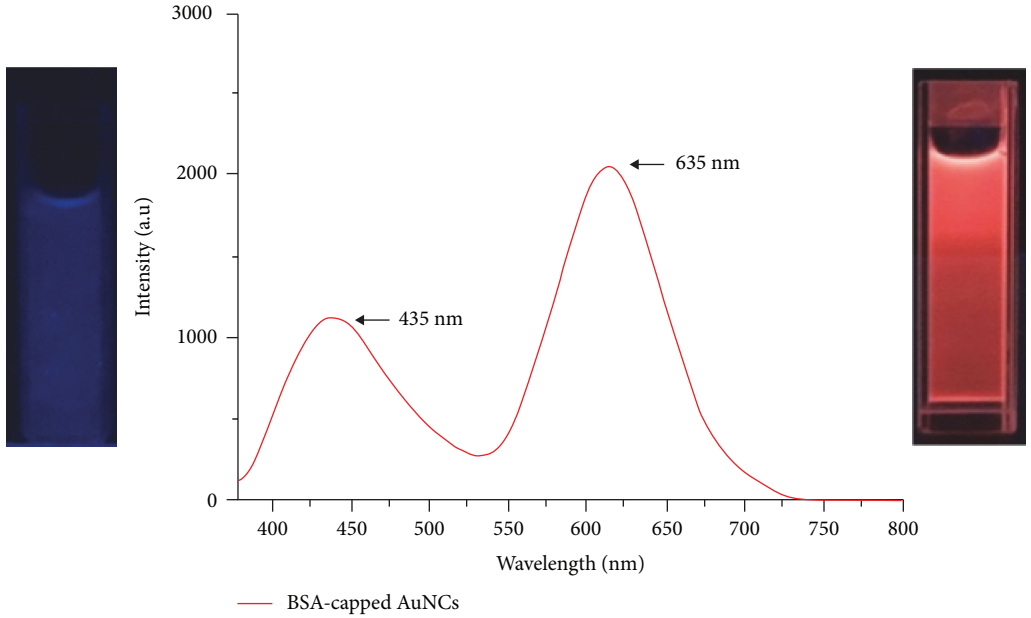

Figure 2: Fluorescence spectrum of BSA-AuNCs. The insert is fluorescence response of BSA (left) and BSA-AuNCs (right) under UV light (365 nm).

characteristic of the aromatic side groups in the amino acid residues (tryptophan, tyrosine (Tyr), and phenylalanine) [27], while the red emission of 635 nm of BSA-AuNCs is contributed to the quantum confinement effect [28, 29]. As confined dimension decreases and reaches a nanoscale, the Fermi level becomes discrete and results in a blue-shift emission. Red fluorescence is emitted when the particles size approaches to 5 nm.

3.2. Antibacterial Experiments of BSA-AuNCs. Before the antibacterial experiments, gold content in BSA-AuNCs was 4.73 mg/l by ICP-MS measurement. In Figure 3, the TKC of BSA-AuNCs against MRSA (ATCC® 33592™), MRSA (ATCC® 49476™), VISA mu3 (ATCC® 700698™), and VISA mu50 (ATCC® 700699™) were formed, respectively. The curves were defined as the absorbance value (OD_{600}) with time, representing the forming of bacterial colony grown in 24 h. The black square symbol lines as the control (-) group described the absorbance value (OD_{600}) of the sterilized TSB solution over time; the absorbance value (OD_{600}) of bacterial solution as the control (+) group is described by the red round symbols; the pink inverse triangle symbol lines described the absorbance value (OD_{600}) of the solution for BSA-added bacteria (BSA/bacterial solution), and the blue triangle symbol lines described the absorbance value (OD_{600}) of the solution for BSA-AuNC-added bacteria (BSA-AuNCs/bacterial solution).

There are important features can be distinguished in the antibacterial experiments. (1) For four bacteria, the absorbance values (OD_{600}) of BSA-AuNCs/bacterial solution at 24 h were all as half lower than that of the normal growth of bacteria. The absorbance value maximum ratios in TKC

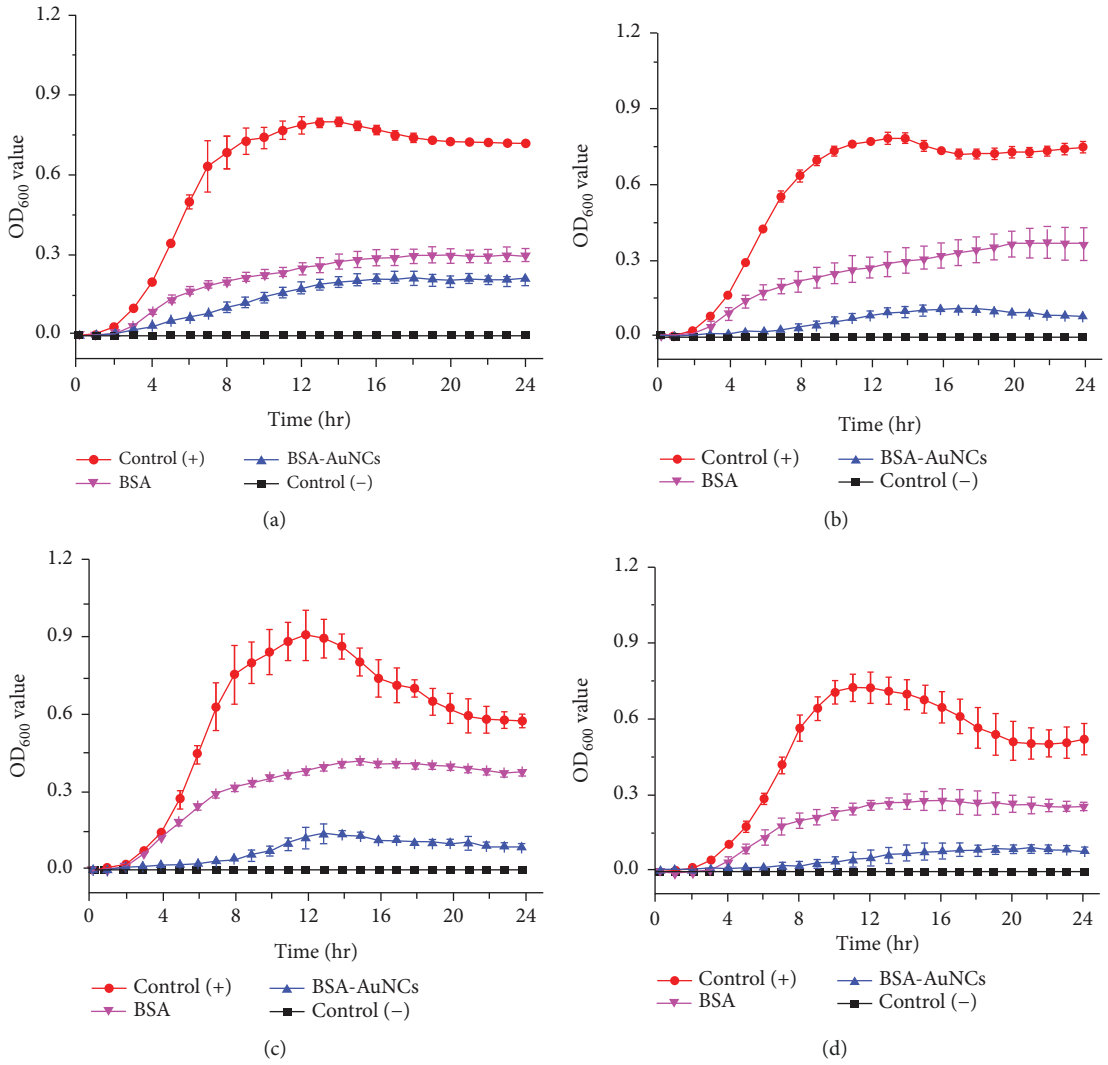

Figure 3: Time-killing curves of BSA-AuNCs against (a) MRSA (ATCC® 33592™), (b) MRSA (ATCC® 49476™), (c) VISA mu3 (ATCC® 700698™), and (d) VISA mu50 (ATCC® 700699™).

of BSA-AuNCs against MRSA (ATCC® 33592™), MRSA (ATCC® 49476™), VISA mu3 (ATCC® 700698™), and VISA mu50 (ATCC® 700699™) vs. the control (+) group were 0.21/0.72, 0.080/0.75, 0.088/0.58, and 0.078/0.52, respectively, as shown in Table 1. The absorbance value (OD_{600}) ranges for BSA-AuNCs/bacterial solution were between 0.07 and 0.22. The absorbance value (OD_{600}) ranges for the normal growth of bacteria were between 0.52 and 0.75. The ratios of the two were between 0.1 and 0.29, indicating that BSA-AuNCs could inhibit about 90%-70% of the bacterial growth. (2) BSA had antibacterial activity to four bacteria, yet BSA-AuNCs performed better on inhibiting bacterial growth since the existence of AuNCs. Comparing to BSA, the folds for BSA-AuNCs in enhanced antibacterial activity are 1.2 times against MRSA (ATCC® 33592™), 4.5 times against MRSA (ATCC® 49476™), 4.3 times against VISA mu3 (ATCC® 700698™), and 3.2 times against VISA mu50 (ATCC® 700699™). (3) BSA-AuNCs/bacterial solution showed antibacterial effect against four bacteria within 4 h. The absorbance values (OD_{600}) of BSA-AuNCs/bacterial solution for four bacteria were slightly changed over time. It showed that its antibacterial effect was stable over time. (4) The curve error bars of MRSA (ATCC® 33592™) and MRSA (ATCC® 49476™) were smaller compared to that of VISA mu3 (ATCC® 700698™) and VISA mu50 (ATCC® 700699™), indicating that the stability of MRSA was better than VISA. The reason might be that VISA was a newer drug resistance gene mutation. (5) The minor curve error bars of BSA-AuNCs in four TKC highlighted superior stability and reproductivity of BSA-AuNCs.

One of the possible antibacterial mechanisms of BSA-AuNCs is BSA was constituted in a hollow cylinder with an open channel, so that small molecules (e.g., reactive oxygen species, ROS) could attack the metal core of the BSA-capped metal nanoparticles, inducing more ROS and inhibiting the bacterial growth [30, 31]. We could speculate the reason of the antibacterial activity from the other metal toxic to bacterial cells, such as Ag. A previous research described that soft metal atoms (such as Au, Ag, Hg, Pt, and Pd) have electron-sharing affinities that can result in the formation

Table 1: The absorbance value maximum (OD_{600} max.) of BSA/bacterial solution, BSA-AuNCs/bacterial solution, and the normal bacteria (control (+) group) against MRSA and VISA.

OD_{600} max.	MRSA (ATCC® 33592™)	MRSA (ATCC® 49476™)	VISA mu3 (ATCC® 700698™)	VISA mu50 (ATCC® 700699™)
BSA/bacterial solution	0.30	0.36	0.38	0.25
BSA-AuNCs/bacterial solution	0.21	0.080	0.088	0.078
Normal bacteria (control (+) group)	0.72	0.75	0.58	0.52

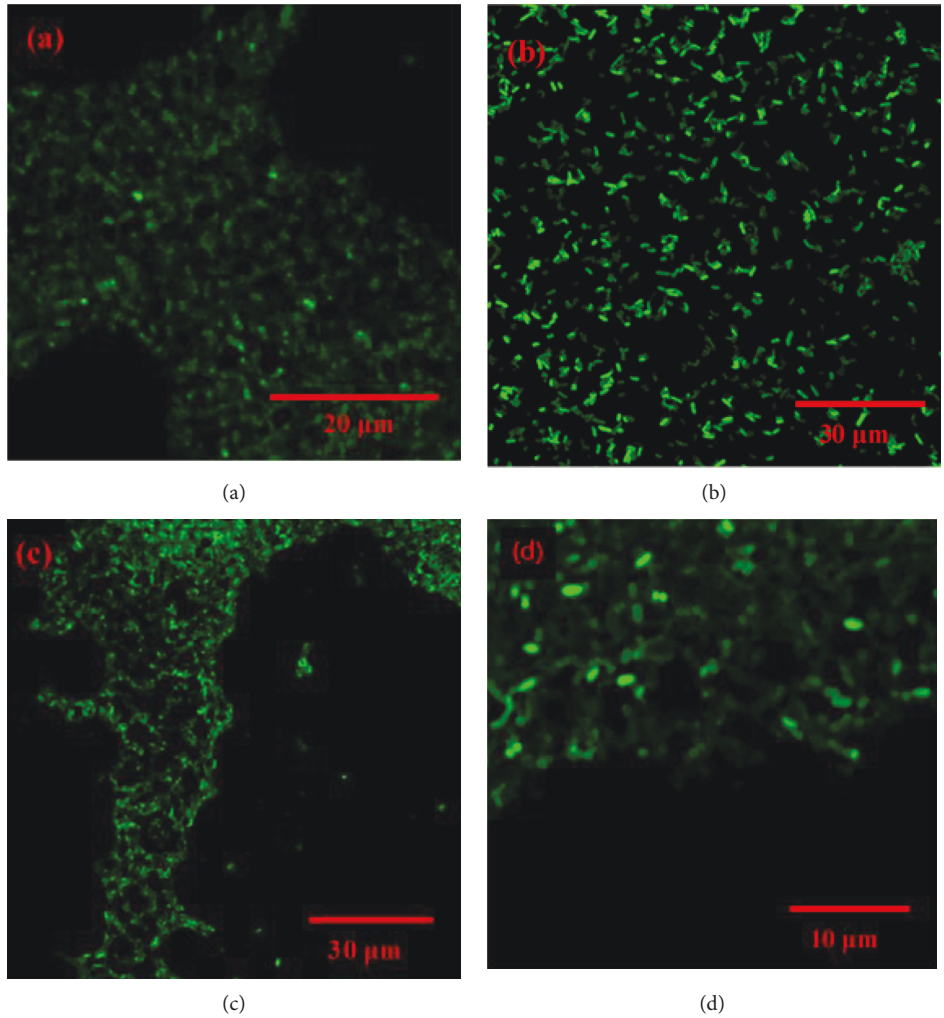

Figure 4: Fluorescence images of (a) VISA mu50, (b) VISA mu50 after treatment with BSA, (c) VISA mu50 after treatment with BSA-AuNCs, and (d) VISA mu3 after treatment with BSA-AuNCs.

of covalent bonds with S in protein, which can lead to the formation of protein dysfunction and the depletion of antioxidant. Aerobic respiration readily gives rise to H_2O_2 and $O_2^{\cdot-}$, and they ultimately lead to bacterial death. H_2O_2 could initiate Au-catalyzed Fenton-like reaction and thus generate more ROS ($^{\cdot}OH$) to intensify O toxicity in bacterial cells [5]. In addition to this, we propose three hypothetical antibacterial mechanisms of BSA-AuNCs: (1) BSA limits the growing space of bacteria and suppresses mitosis of bacteria, (2) gold nanoparticles have positive surface charge and could enhance BSA to attach to the negatively charged surface of the bacteria, and (3) gold ions could penetrate the bacterial wall, which interrupts the metabolic pathway of bacteria.

3.3. Fluorescence Images of Bacteria. In order to confirm the possible antibacterial mechanisms of BSA-AuNCs against VISA, we used cLSM for direct observation. A fluorescence image of VISA mu50 in Figure 4(a) shows that it is a normal bacterial growth and the shape of the bacteria is complete and smooth, well dispersed, and no obvious aggregation or deformation. A fluorescence image of VISA mu50 after treatment with BSA in Figure 4(b) shows that the bacteria are deformed and there is a phenomenon of agglomeration. A fluorescence

image of VISA mu50 after treatment with BSA-AuNCs in Figure 4(c) shows that the bacteria are deformed and there is a phenomenon of agglomeration, which is similar with Figure 4(b). A fluorescence image of VISA mu3 is similar with Figure 4(a) and shows that it is a normal bacterial growth, the shape of the bacteria is complete and smooth, well dispersed, and no obvious aggregation or deformation. A fluorescence image of VISA mu3 after treatment with BSA is similar with Figure 4(b) and shows that the bacteria are deformed and there is a phenomenon of agglomeration. A fluorescence image of VISA mu3 after treatment with BSA-AuNCs in Figure 4(d) shows that the bacteria are deformed and there is a phenomenon of agglomeration, which is similar with the fluorescence image of VISA mu3 after treatment with BSA. The fluorescence images of VISA mu50 and VISA mu3 under cLSM are similar; the appearances of the bacteria remained complete and were well distributed. After treatment with BSA (0.1 wt%) onto VISA mu50 and VISA mu3, the bacteria aggregated apparently and became nonspherical, which were attributed to growth suppression by BSA. However, the fluorescence image of VISA mu3/VISA mu50 after treatment with BSA is similar with the fluorescence image of VISA mu3/VISA mu50 after treatment with BSA-AuNCs. Gold nanoparticles did not cause significant damage to the bacterial membrane, yet only from the images; it could not prove itself whether AuNCs interrupted the metabolic pathway in bacterial cell. However, owing to the shape of bacteria changed, it suggested that the induced ROS could attack the bacteria, which was majorly contributed to the growth inhibition. We also find from Figure 4 that the effect of BSA on bacterial growth is similar to the hypothetical antibacterial mechanism (1), due to the deformation of the bacteria. After treatment with BSA or BSA-AuNCs, the fluorescence images look similar. They are deformed and agglomerated, especially the phenomenon of agglomeration which might be caused by the hypothetical antibacterial mechanism (2) that AuNCs can pull BSA closer to the bacteria to cause compression. The antibacterial mechanism of BSA-AuNCs that can help inhibit the bacterial growth might also be BSA limits the growing space of bacteria and suppresses mitosis of bacteria and gold nanoparticles have positively charged surface and could enhance BSA to attach to the negatively charged surface of the bacteria. A biochemical pathway cannot be known from the images, so it is not possible to directly prove the hypothetical antibacterial mechanism (3).

4. Conclusions

In this study, BSA-AuNCs were prepared by green synthesis. The results of the experiment are summarized as follows:

(1) TEM images indicated that the AuNCs were well encapsulated in BSA. The shape of the AuNCs was spherical, and the average diameter was about 5 nm

(2) In fluorescence spectra, the blue-emitting BSA presented a weak broad band at 435 nm and BSA-AuNCs emitted an intense red fluorescence at 635 nm

(3) BSA-AuNCs could inhibit about 90%-70% of the bacterial growth, which is proved by TKC. The gold content of BSA-AuNCs in the antibacterial experiments was 4.73 mg/l by ICP-MS measurement

(4) The major antibacterial mechanism in this study was ROS could attack the metal core of the BSA-AuNCs, generating more ROS to prejudice bacterial growth

(5) The hypothetical antibacterial mechanism (1) was consistent with the result of the fluorescence images. Due to limitations of analytical techniques, the hypothetical antibacterial mechanism (2) was not confirmed. It was possible that the greater antibacterial activity of BSA-AuNCs was contributed to the released gold and gold ions interacting the functional compounds of bacterial cells

Data Availability

The data used to support the findings of this study are available from the corresponding author upon request.

Conflicts of Interest

The authors declare that they have no conflicts of interest.

Authors' Contributions

Shu-Hua Kuo and Chi-Sheng Chien contributed equally to this work.

Acknowledgments

The authors acknowledge the support of grants from the Chi-Mei Medical Center and Kaohsiung Medical University Research Foundation (107CM-KMU-07) and the Research Project of Ministry of Science and Technology of Taiwan (MOST 104-2221-E-037-003-MY3).

References

[1] J. Carlet, P. Collignon, D. Goldmann et al., "Society's failure to protect a precious resource: antibiotics," *The Lancet*, vol. 378, no. 9788, pp. 369–371, 2011.

[2] P. Nordmann, T. Naas, N. Fortineau, and L. Poirel, "Superbugs in the coming new decade; multidrug resistance and prospects for treatment of Staphylococcus aureus, Enterococcus spp. and Pseudomonas aeruginosa in 2010," *Current Opinion in Microbiology*, vol. 10, no. 5, pp. 436–440, 2007.

[3] B. Spellberg, R. Guidos, D. Gilbert et al., "The epidemic of antibiotic-resistant infections: a call to action for the medical community from the Infectious Diseases Society of America," *Clinical Infectious Diseases*, vol. 46, no. 2, pp. 155–164, 2008.

[4] M. Bassetti, M. Merelli, C. Temperoni, and A. Astilean, "New antibiotics for bad bugs: where are we?," *Annals of Clinical Microbiology and Antimicrobials*, vol. 12, no. 1, p. 22, 2013.

[5] J. A. Lemire, J. J. Harrison, and R. J. Turner, "Antimicrobial activity of metals: mechanisms, molecular targets and applications," *Nature Reviews Microbiology*, vol. 11, no. 6, pp. 371–384, 2013.

[6] E. E. Connor, J. Mwamuka, A. Gole, C. J. Murphy, and M. D. Wyatt, "Gold nanoparticles are taken up by human cells but do not cause acute cytotoxicity," *Small*, vol. 1, no. 3, pp. 325–327, 2005.

[7] Y. S. Chen, Y. C. Hung, I. Liau, and G. S. Huang, "Assessment of the in vivo toxicity of gold nanoparticles," *Nanoscale Research Letters*, vol. 4, no. 8, pp. 858–864, 2009.

[8] V. Kattumuri, K. Katti, S. Bhaskaran et al., "Gum Arabic as a phytochemical construct for the stabilization of gold nanoparticles: in vivo pharmacokinetics and X-ray-contrast-imaging studies," *Small*, vol. 3, no. 2, pp. 333–341, 2007.

[9] J. Cao, T. Sun, and K. T. V. Grattan, "Gold nanorod-based localized surface plasmon resonance biosensors: a review," *Sensors and Actuators B: Chemical*, vol. 195, pp. 332–351, 2014.

[10] P. A. Rasheed and N. Sandhyarani, "Electrochemical DNA sensors based on the use of gold nanoparticles: a review on recent developments," *Microchimica Acta*, vol. 184, no. 4, pp. 981–1000, 2017.

[11] P. Mehrotra, "Biosensors and their applications–a review," *Journal of Oral Biology and Craniofacial Research*, vol. 6, no. 2, pp. 153–159, 2016.

[12] S. H. Brorson, "Bovine serum albumin (BSA) as a reagent against non-specific immunogold labeling on LR-White and epoxy resin," *Micron*, vol. 28, no. 3, pp. 189–195, 1997.

[13] Y. Wang, Y. Wu, Y. Liu et al., "BSA-mediated synthesis of bismuth sulfide nanotheranostic agents for tumor multimodal imaging and thermoradiotherapy," *Advanced Functional Materials*, vol. 26, no. 29, pp. 5335–5344, 2016.

[14] F. Vollmer, D. Braun, A. Libchaber, M. Khoshsima, I. Teraoka, and S. Arnold, "Protein detection by optical shift of a resonant microcavity," *Applied Physics Letters*, vol. 80, no. 21, pp. 4057–4059, 2002.

[15] A. Rösler, G. W. M. Vandermeulen, and H. A. Klok, "Advanced drug delivery devices via self-assembly of amphiphilic block copolymers," *Advanced Drug Delivery Reviews*, vol. 64, pp. 270–279, 2012.

[16] A. Aires, S. M. Ocampo, D. Cabrera et al., "BSA-coated magnetic nanoparticles for improved therapeutic properties," *Journal of Materials Chemistry B*, vol. 3, no. 30, pp. 6239–6247, 2015.

[17] S. Iravani, "Green synthesis of metal nanoparticles using plants," *Green Chemistry*, vol. 13, no. 10, pp. 2638–2650, 2011.

[18] N. R. Jana, L. Gearheart, and C. J. Murphy, "Seed-mediated growth approach for shape-controlled synthesis of spheroidal and rod-like gold nanoparticles using a surfactant template," *Advanced Materials*, vol. 13, no. 18, pp. 1389–1393, 2001.

[19] D. Philip, "Honey mediated green synthesis of gold nanoparticles," *Spectrochimica Acta Part A: Molecular and Biomolecular Spectroscopy*, vol. 73, no. 4, pp. 650–653, 2009.

[20] J. M. Andrews, "Determination of minimum inhibitory concentrations," *Journal of Antimicrobial Chemotherapy*, vol. 48, Supplement_1, pp. 5–16, 2001.

[21] J. Xie, Y. Zheng, and J. Y. Ying, "Protein-directed synthesis of highly fluorescent gold nanoclusters," *Journal of the American Chemical Society*, vol. 131, no. 3, pp. 888-889, 2009.

[22] L. Dong, M. Li, S. Zhang et al., "Cytotoxicity of BSA-stabilized gold nanoclusters: in vitro and in vivo study," *Small*, vol. 11, no. 21, pp. 2571–2581, 2015.

[23] S. Govindaraju, S. R. Ankireddy, B. Viswanath, J. Kim, and K. Yun, "Fluorescent gold nanoclusters for selective detection of dopamine in cerebrospinal fluid," *Scientific Reports*, vol. 7, no. 1, article 40298, 2017.

[24] N. Y. Hsu and Y. W. Lin, "Microwave-assisted synthesis of bovine serum albumin–gold nanoclusters and their fluorescence-quenched sensing of Hg^{2+} ions," *New Journal of Chemistry*, vol. 40, no. 2, pp. 1155–1161, 2016.

[25] Y. Chang, Z. Zhang, J. Hao, W. Yang, and J. Tang, "BSA-stabilized Au clusters as peroxidase mimetic for colorimetric detection of Ag+," *Sensors and Actuators B: Chemical*, vol. 232, pp. 692–697, 2016.

[26] J. Huang, J. Zhou, J. Zhuang et al., "Strong near-infrared absorbing and biocompatible CuS nanoparticles for rapid and efficient photothermal ablation of gram-positive and -negative bacteria," *ACS Applied Materials & Interfaces*, vol. 9, no. 42, pp. 36606–36614, 2017.

[27] L. Hu, S. Han, S. Parveen, Y. Yuan, L. Zhang, and G. Xu, "Highly sensitive fluorescent detection of trypsin based on BSA-stabilized gold nanoclusters," *Biosensors and Bioelectronics*, vol. 32, no. 1, pp. 297–299, 2012.

[28] S. Eustis and M. A. El-Sayed, "Why gold nanoparticles are more precious than pretty gold: noble metal surface plasmon resonance and its enhancement of the radiative and nonradiative properties of nanocrystals of different shapes," *Chemical Society Reviews*, vol. 35, no. 3, pp. 209–217, 2006.

[29] O. Varnavski, G. Ramakrishna, J. Kim, D. Lee, and T. Goodson, "Critical size for the observation of quantum confinement in optically excited gold clusters," *Journal of the American Chemical Society*, vol. 132, no. 1, pp. 16-17, 2010.

[30] K. Murayama and M. Tomida, "Heat-induced secondary structure and conformation change of bovine serum albumin investigated by Fourier transform infrared spectroscopy," *Biochemistry*, vol. 43, no. 36, pp. 11526–11532, 2004.

[31] J. Huang, L. Lin, D. Sun, H. Chen, D. Yang, and Q. Li, "Bio-inspired synthesis of metal nanomaterials and applications," *Chemical Society Reviews*, vol. 44, no. 17, pp. 6330–6374, 2015.